The American Journal of Human Genetics, Volume *107*

Supplemental Data

A Recurrent Gain-of-Function Mutation in *CLCN6*, Encoding the ClC-6 Cl^-/H^+-Exchanger, Causes Early-Onset Neurodegeneration

Maya M. Polovitskaya, Carlo Barbini, Diego Martinelli, Frederike L. Harms, F. Sessions Cole, Paolo Calligari, Gianfranco Bocchinfuso, Lorenzo Stella, Andrea Ciolfi, Marcello Niceta, Teresa Rizza, Marwan Shinawi, Kathleen Sisco, Jessika Johannsen, Jonas Denecke, Rosalba Carrozzo, Daniel J. Wegner, Kerstin Kutsche, Marco Tartaglia, and Thomas J. Jentsch

SUPPLEMENTAL DATA

Case Reports

Subject 1

Patient 1 was the 4th child of Bulgarian healthy parents with negative family history. No problems were reported during pregnancy and at birth. At the age of 5 months, during an episode of bronchiolitis, he had two cardiac arrests and severe respiratory failure requiring intubation and tracheostomy. A first brain MRI showed mild bilateral fronto-temporal cerebral atrophy. EEG documented frontal epileptic abnormalities. At 7 months, clinical examination documented severe developmental delay, wandering movements of the eyes, generalized hypotonia, insensitivity to pain, hyperhidrosis, presence of gastrostomy and neurogenic bladder. The second brain MRI at age 10 months showed a progression of cortical atrophy, bilateral fronto-parietal subdural chronic hematomas and bilateral symmetrical abnormalities at level of corticospinal tracts, in correspondence of the cerebral peduncles, substantia nigra and thalami, with restricted diffusivity at DWI. VEPs revealed an increase of latency and abnormal morphology of P100 wave. Sensory peripheral neuropathy was detected by nerve conduction assessment. An extensive metabolic workup documented persistent low serum copper (5-12 µg/dl; n.v. 83-180), low-normal ceruloplasmin (24-26 mg/dl, n.v. 20-40), and low urinary copper excretion over 24h (15.4 µg/24h, n.v. 15-70). Zinc level was normal. Additional abnormalities included increase of plasma alanine and creatine, with normal blood lactate, VLCFA, guanidine acetic acid, urinary organic acids. Kayser–Fleischer ring was excluded by ophthalmologic examination. Hair microscopy study documented trichorrhexis nodosa, with reduced hair copper content at atomic emission spectrometry/inductively coupled plasma mass spectrometry (8.1 mg/1000g, n.v. 12.0-30.0). Ultrasound scan disclosed bladder diverticula. Skin biopsy study documented abnormal elastic fibers. In muscle biopsy, mild signs of myopathy were observed, but spectrophotometric measurement of respiratory chain complexes activities was inconclusive due to lack of muscle. Clinical and biochemical abnormalities prompted to suspect a copper metabolism disorder. Karyotype, array-CGH, and targeted exon sequencing of known genes implicated in copper metabolism disorders (*ATP7A*, *ATP7B*, *SLC33A1*, *CCS*, *AP1B1* and *AP1S1*) did not reveal the occurrence of pathogenic variants. At 4 years of age, the patient presented two paroxystic episodes, characterized by staring, hypertonia, and desaturation, lasting 5 minutes, and resolved after administration of oxygen therapy. A slight raise of serum copper level, without normalization (62.6 µg /dl) was observed under enteral copper salt administration. At the last examination (6y 4m), the patient showed severe developmental delay, tetraplegia, cortical blindness, complete absence of language and spontaneous movements, chronic respiratory insufficiency requiring continuous invasive ventilation. Based on the negative molecular findings the patient was enrolled in the “Undiagnosed Patient Program” at the Ospedale Pediatrico Bambino Gesù (Rome, Italy), and WES was performed using a trio-based approach.

Subject 2

She was the first child of healthy, non-consanguineous parents of European descent. Birth was at 39 + 6 weeks of gestation by normal vaginal delivery. The mother had a history of two previous spontaneous miscarriages and one induced abortion due to trisomy 21. During pregnancy decreased fetal movements were noted. Weight, length and occipital frontal circumference at birth were in the normal range. At first examination, the 3-month-old girl presented with severe muscular hypotonia, moderate global developmental delay and failure to thrive due to feeding difficulties. Eye contact and hearing appeared to be normal. Eight weeks later, further diagnostic work-up, including extensive metabolic

investigations in blood, urine and cerebrospinal fluid, revealed normal results. Brain MRI at the age of 5 months and 6 months was normal. After the first brain MRI in sedation with chloral hydrate the patient developed prolonged sedation and hypopnea requiring mechanical ventilation. Then, non-invasive ventilation during sleep was necessary because of persistent hypoventilation. Chromosome analysis and array CGH revealed normal results. Genetic testing for spinal muscular atrophy, facioscapulohumeral muscular dystrophy, myotonic dystrophy type 1, and Prader-Willi syndrome also was normal. At 13 months of age, the girl was able to roll over but could not sit or crawl, spoke single words, showed poor eye contact, decreased facial expression and abnormal involuntary eye movements. Muscular tone and reflexes were severely reduced or absent, and she exhibited mild dyskinesia. Multiple café-au-lait spots and axillar freckling but not the severe and progressive neurological symptoms were in line with genetically confirmed neurofibromatosis type 1. After the age of 16 months, she showed global deterioration with constant respiratory insufficiency, psychomotor and neurodevelopmental regression, intermittent severe choreoathetoid and dyskinetic movement disorder, abnormality of temperature regulation, hyperhidrosis, and neurogenic bladder. Gastrostomy tube feeding became necessary, and tracheostomy was performed for invasive ventilation. Brain MRI at the age of 18 months documented mild cerebral atrophy and symmetrical diffusion restriction in the upper cerebellar peduncles and dorsal brainstem. Initial EEG was normal but generalized slowing developed during the course of the disease. In muscle biopsy, mild signs of myopathy as well as subsarcolemmal accumulation of mitochondria and fatty vacuoles were identified. Copper metabolism was not examined. At the age of 23 months, the girl died due to pneumonia and fatal respiratory insufficiency.

Subject 3

The proband, a 22-month-old female of European descent, was the only child of apparently unrelated parents. Her mother had a previous spontaneous abortion at 7 weeks of gestation, and had a history of epilepsy, controlled with medications. There is no family history of birth defects, recurrent miscarriages, early infant deaths, or intellectual disability.

The Proband had a history of hypotonia and developmental delay and is currently tracheostomy and ventilator dependent. At 5 months of age, she started having cyanotic spells with large gasp about 2-3 times per week. At 7 months, she had a prolonged episode of apnea followed by “choking coughs" and was noted to have significant hypotonia, for which she was admitted to the hospital for further work up. During her admission, the proband failed extubation after a sedated brain MRI, leading to an extensive workup and admission for 2 ½ months. She has been tracheostomy and ventilator dependent since she was 7 month-old. She also had a gastrostomy tube placed but removed after 3 months when she resumed full feeding. After her discharge from the hospital, the proband started regressing in her developmental milestones and exhibiting global developmental delay, for which she started receiving physical, speech and developmental therapy. She was able to sit without support at 14 months but does not crawl, stand or walk at 22 months. She can finger feed herself but is not able to use utensils. She can verbalize 7-8 single words and recognize 5-6 signs.

On physical examination at 23 months of age, her weight was at the 7th percentile (Z= -1.5), length below 1st percentile (Z= -3.3). At 19 months, her occipitofrontal circumference (OFC) was at 59th percentile (Z= 0.24). She was alert, in no acute distress, and occasionally smiled and laughed. Her tracheostomy tube was in place. She had no major dysmorphic features. Ophthalmological exam showed bilateral optic disc fullness, tenting of overlying neural tissue and “sandcastle” appearance of

optic nerves with some improvement between 19 and 23 months. She had alternating esotropia (right>left) and strabismic amblyopia associated with head tilting. Her neurological exam was significant for generalized hypotonia, truncal more than peripheral, asymmetric face with droopy mouth on the left when smiling, and absent reflexes in lower limbs.

Her diagnostic workup included brain MRI when she was 7 months old, which showed symmetric areas of diffusion restriction involving bilateral cerebral peduncles, dorsal midbrain and inferiorly along the dorsal aspect of the pons and medulla, with mild T2 hyperintensity. MRI orbits significant for soft tissue thickening and elevation of the optic discs bilaterally and mild enhancement of the optic nerve sheaths. Repeated MRI/MRS at 23 mo showed improved diffusion restriction with small persistent foci of restricted diffusion in the bilateral anteromedial cerebral peduncles. There was no evidence of lactate peak but small GIX peak was present. Echocardiography was normal. Her video EEG was negative for seizures. Hearing evaluation was unremarkable. Diaphragm fluoroscopy showed normal movement of both hemidiaphragms. Electromyography (EMG) and pyridostigmine tests at 8 mo were unremarkable. Nerve condition studies and repeated EMG at 22 months were normal. Muscle biopsy was also performed, and immunohistochemistry showed abnormal variation in muscle fiber sizes with many scattered very small type II muscle fibers. Sleep study at 8 months showed short frequent central apneas, 13 per hour, but with rapid falls in saturations to the 70s. Sleep study at 19 months with a tracheostomy in place did not suggest a central problem with ventilatory control. However, the desaturations with short central apnea would suggest poor lung volume maintenance that would be consistent with her hypotonia. Urine organic acid analysis initially showed moderate elevation of pyroglutamate but repeated testing was normal. Total and free carnitine as well as acylcarnitine profile were normal. She had elevation of multiple amino acids, especially the neutral amino acids, in the urine, which can reflect renal tubular dysfunction or Hartnup disease. Plasma amino acids in blood and CSF showed nonspecific low levels of several amino acids but were essentially normal in repeat testing. Lysosomal enzymes were normal. The concentrations of neurotransmitter metabolites in CSF were within reference ranges. Serum copper and ceruloplasmin were normal. Zinc was below the normal range (0.58; nl: 0.60 - 1.20 µ/mL). Thyroid function studies, CK, and homocysteine levels were normal. Chromosomal microarray analysis, mtDNA sequencing and deletion/duplication, and *PHOX2B* sequencing were negative. The patient was enrolled in the "Undiagnosed Diseases Network (UDN)" (https://undiagnosed.hms.harvard.edu/) supported by the National Human Genome Research Institute of the National Institutes of Health.

Supplemental Figures

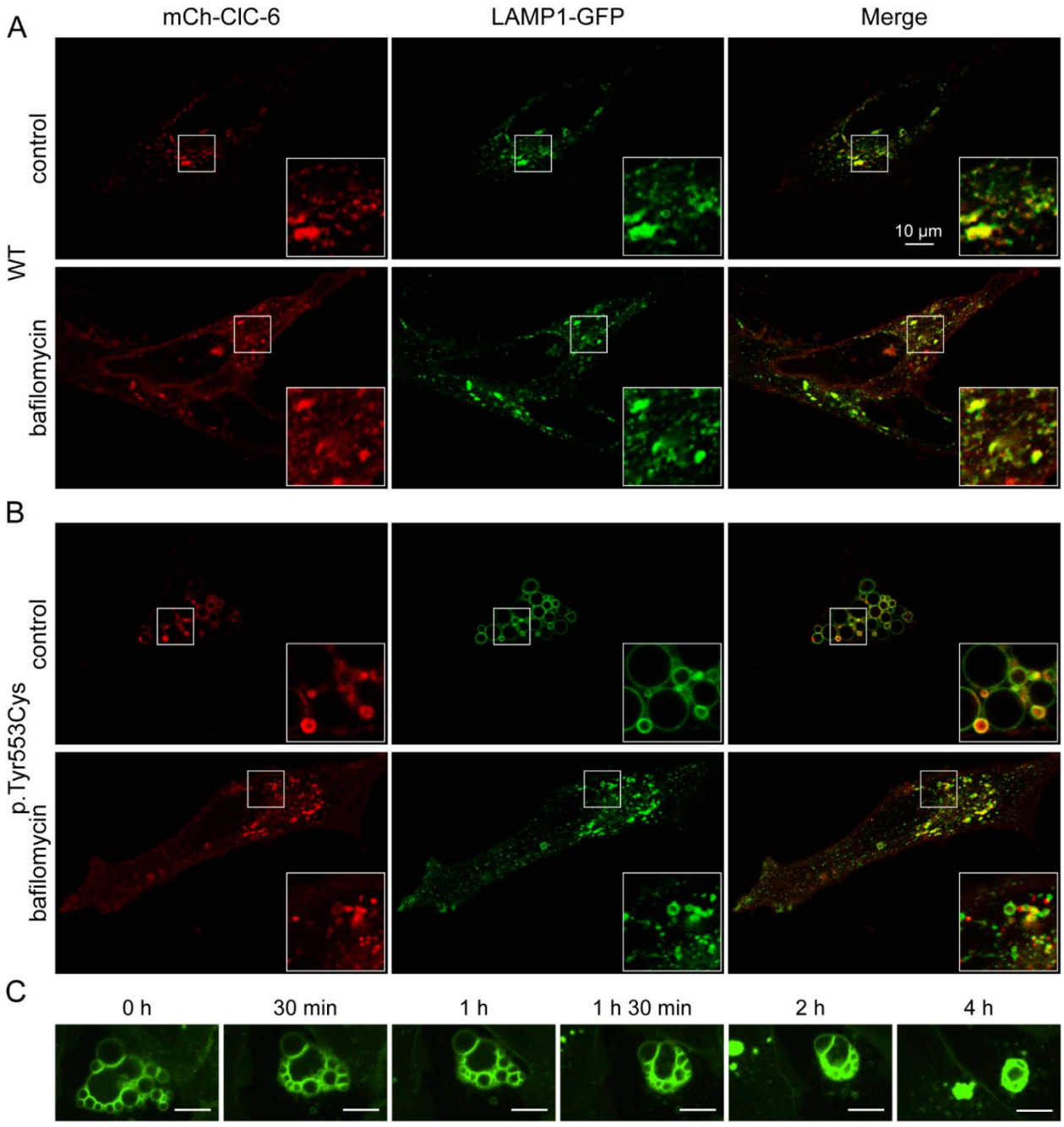

Figure S1. Generation of large vesicles by ClC-6^{Tyr553Cys} overexpression is prevented by bafilomycin. HeLa cells were co-transfected with LAMP1-GFP and either mCherry-ClC-6 (**A**) or mCherry-ClC-6^{Tyr553Cys} (**B**), and imaged after 24 h, either in normal conditions or upon treatment with 10 nM bafilomycin, which was added 4 h after transfection. Note that bafilomycin treatment impaired formation of LAMP1-positive vacuoles by ClC-6^{Tyr553Cys}. (**C**) Selected frames from a live cell imaging video (Video S3) showing shrinkage of giant vesicles in U2OS LAMP1-GFP cells transfected with ClC-6^{Tyr553Cys}. Scale bar, 10 µm.

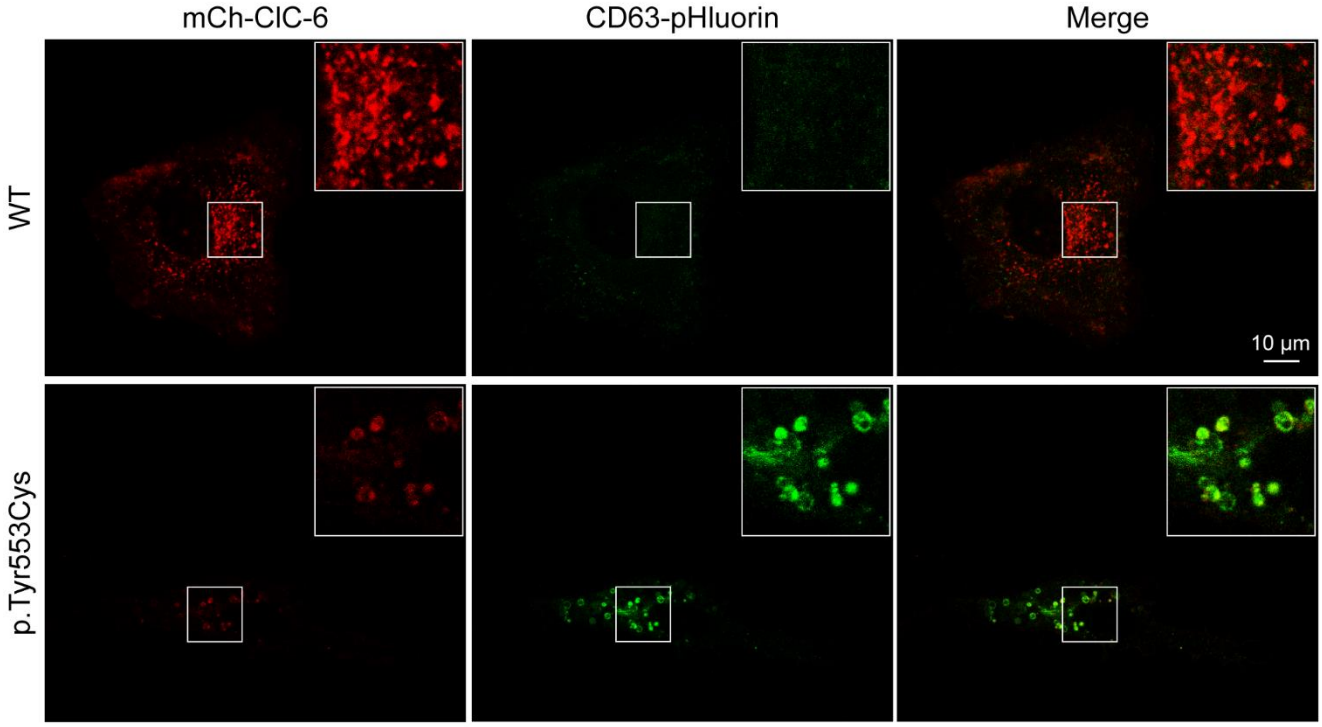

Figure S2. Vacuoles formed by mCherry-ClC-6^{Tyr553Cys} show CD63-pHluorin fluorescence. HeLa cells were transfected with mCherry-labeled WT or p.Tyr553Cys ClC-6 together with the pH-sensitive CD63-pHluorin, which fluoresces only close to neutral pH. Note that CD63-pHluorin co-localizes with the membrane of enlarged vesicles when the mutant is transfected, but not with the mCherry WT ClC-6-containing vesicles.

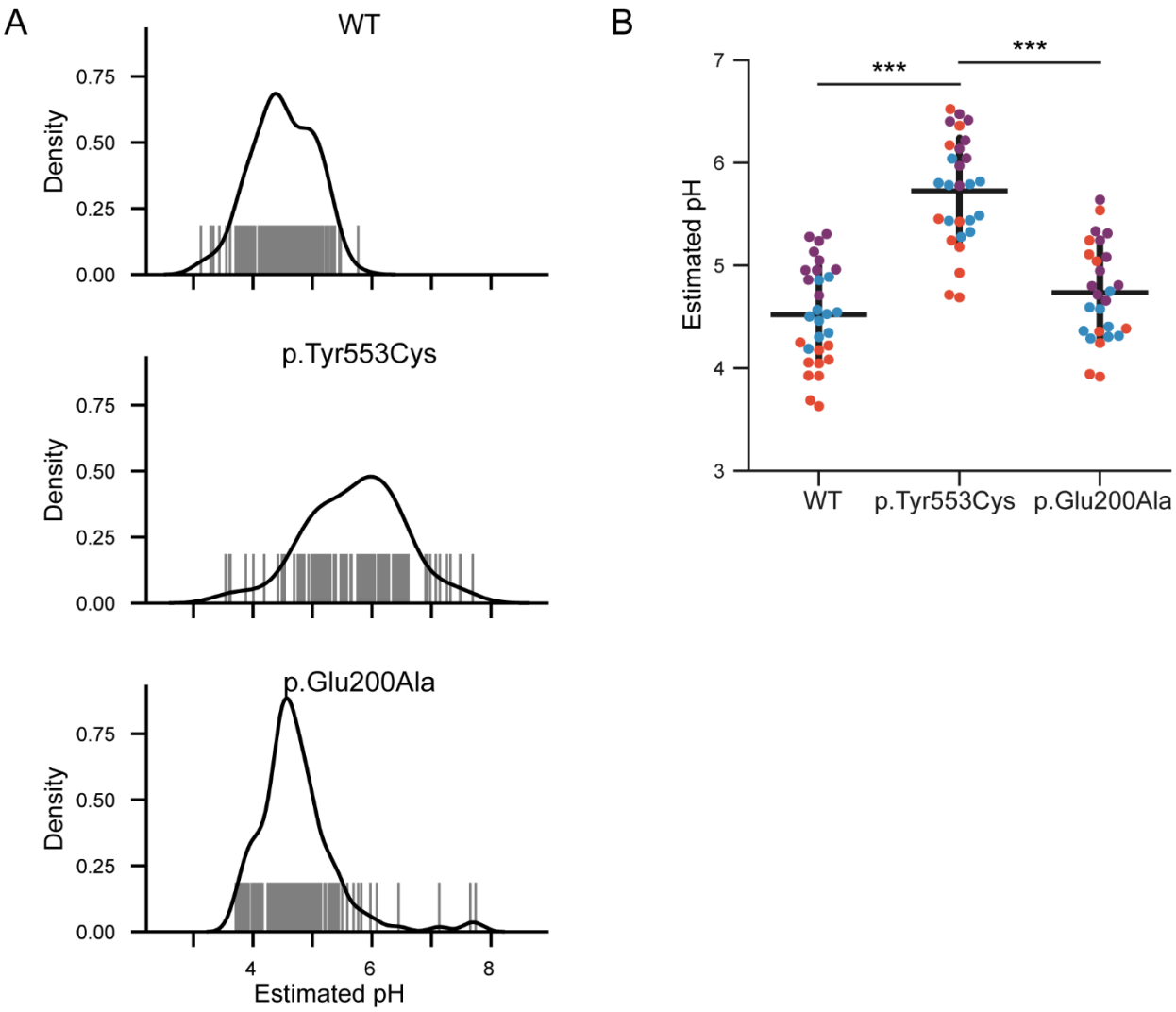

Figure S3. Less acidic vesicular pH in ClC-6^{Tyr553Cys} transfected cells. HeLa cells were transfected either with ClC-6^{WT}, ClC-6^{Tyr553Cys} or ClC-6^{Glu200Ala}, loaded overnight with OregonGreen 488 Dextran, and imaged after a 2 h chase in complete medium. Intracellular compartments showing OregonGreen 488 fluorescence were manually chosen as regions of interests, and fluorescence intensities were measured with alternating excitation at λ = 488 and 440 nm. The fluorescence ratio was converted to pH using equilibration of cells with different values of extracellular pH in the presence of ionophores. Co-transfection of a pmRFP reporter was used to confirm transfection. (**A**) Gray bars indicate the estimated pH values of individual vesicles in cells transfected either with ClC-6^{WT}, ClC-6^{Tyr553Cys} or ClC-6^{Glu200Ala}. Solid line represents Gaussian kernel density estimate of the probability density function of vesicular pH. (**B**) Estimated vesicular pH for individual cells. Each dot is an average over all vesicles in one cell, color indicates three independent experiments. Note that ClC-6^{Tyr553Cys} transfected cells displayed an average pH of ~5.8 ± 0.4, whereas WT and p.Glu200Ala mutants displayed an average pH of ~4.5 ± 0.5 and ~4.7 ± 0.3, respectively. Horizontal line, mean; error bars, SD; ***, p<0.001 (Tukey post hoc test for linear mixed model with vesicular pH as the dependent variable, genotype as a fixed effect and replicate as a random effect).

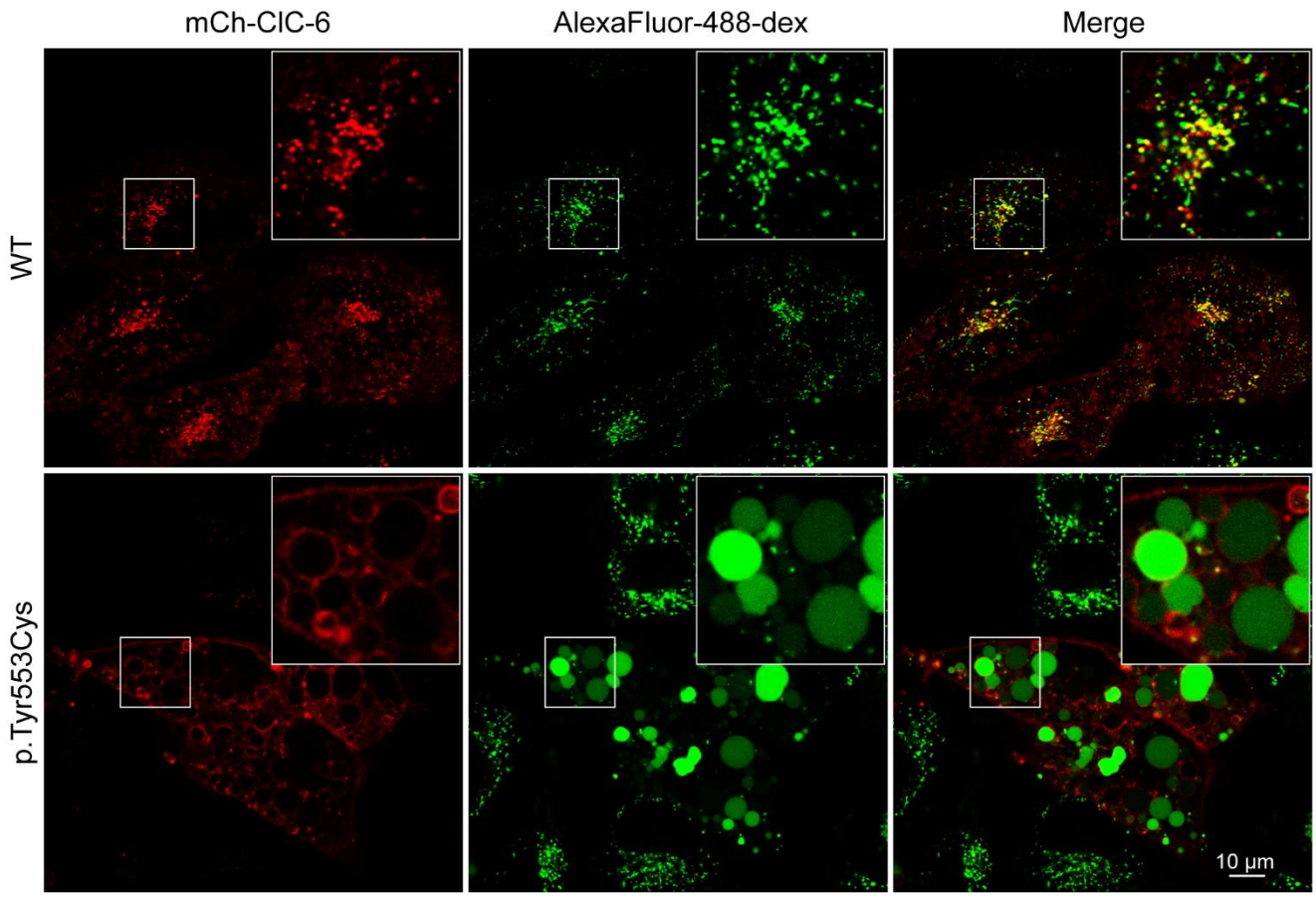

Figure S4. Vacuoles formed by ClC-6^{Tyr553Cys} accumulate endocytic cargo to different degrees. HeLa cells were transfected with WT or p.Tyr553Cys ClC-6, both tagged at the N-terminus with mCherry, and labeled by overnight endocytic uptake and a subsequent 2 h chase with Alexa-Fluor-488 dextran. Endocytosed fluorescently labeled dextran labels the entire lumen of some vesicles, whereas others are only weakly labeled or appear devoid of dextran.

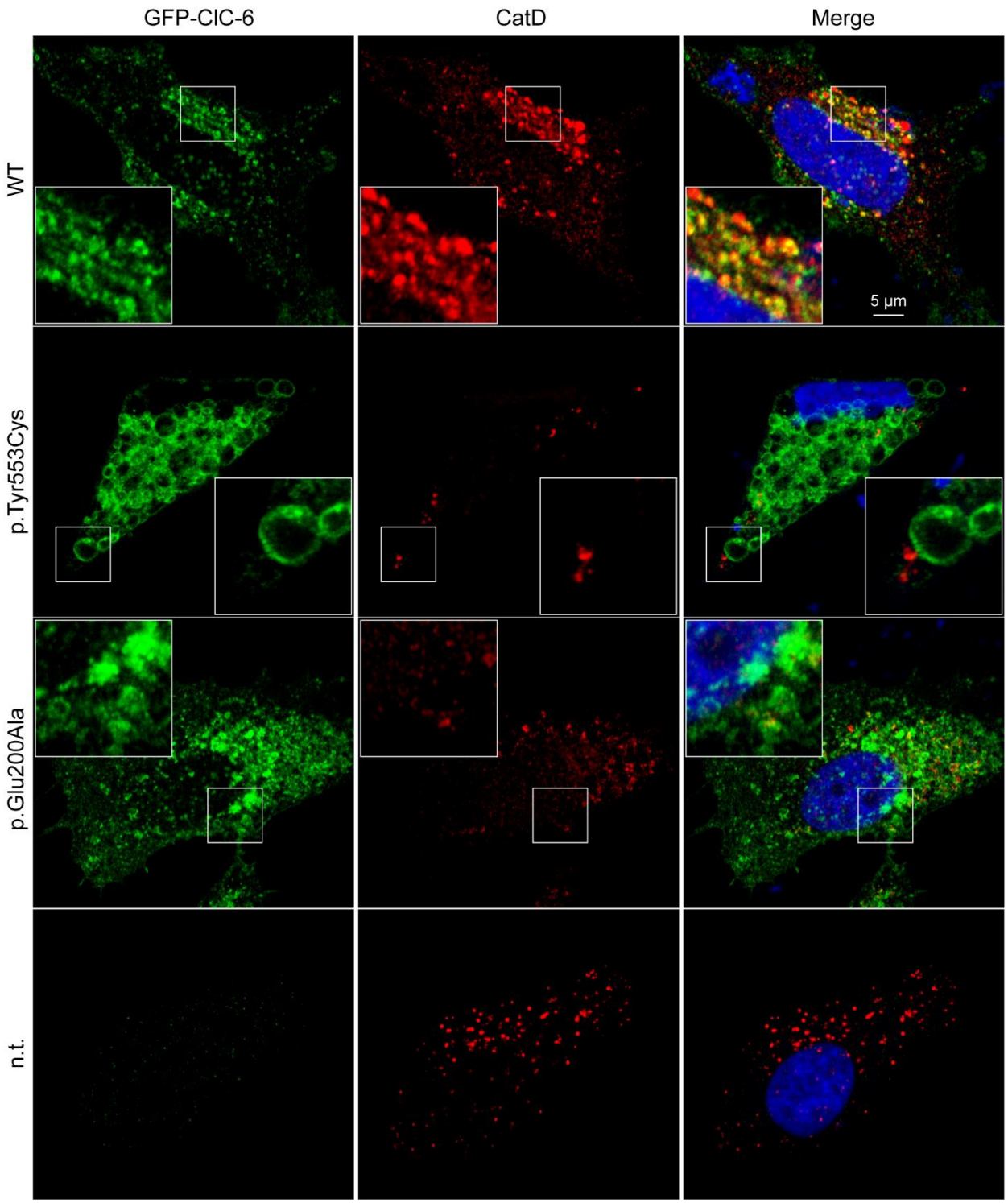

Figure S5. Cathepsin D does not localize to vesicles generated by overexpression of ClC-6 mutants. HeLa cells were transfected with ClC-6^{WT}, ClC-6^{Tyr553Cys}, ClC-6^{Glu200Ala}, or non-transfected. ClC-6 partially co-localized with cathepsin D (CatD) in WT transfected cells, but not in cells transfected with either the p-Tyr553Cys or the p.Glu200Ala mutant. ClC-6 mutant-expressing cells appear to contain less cathepsin D. All ClC-6 constructs had GFP fused to the N-terminus.

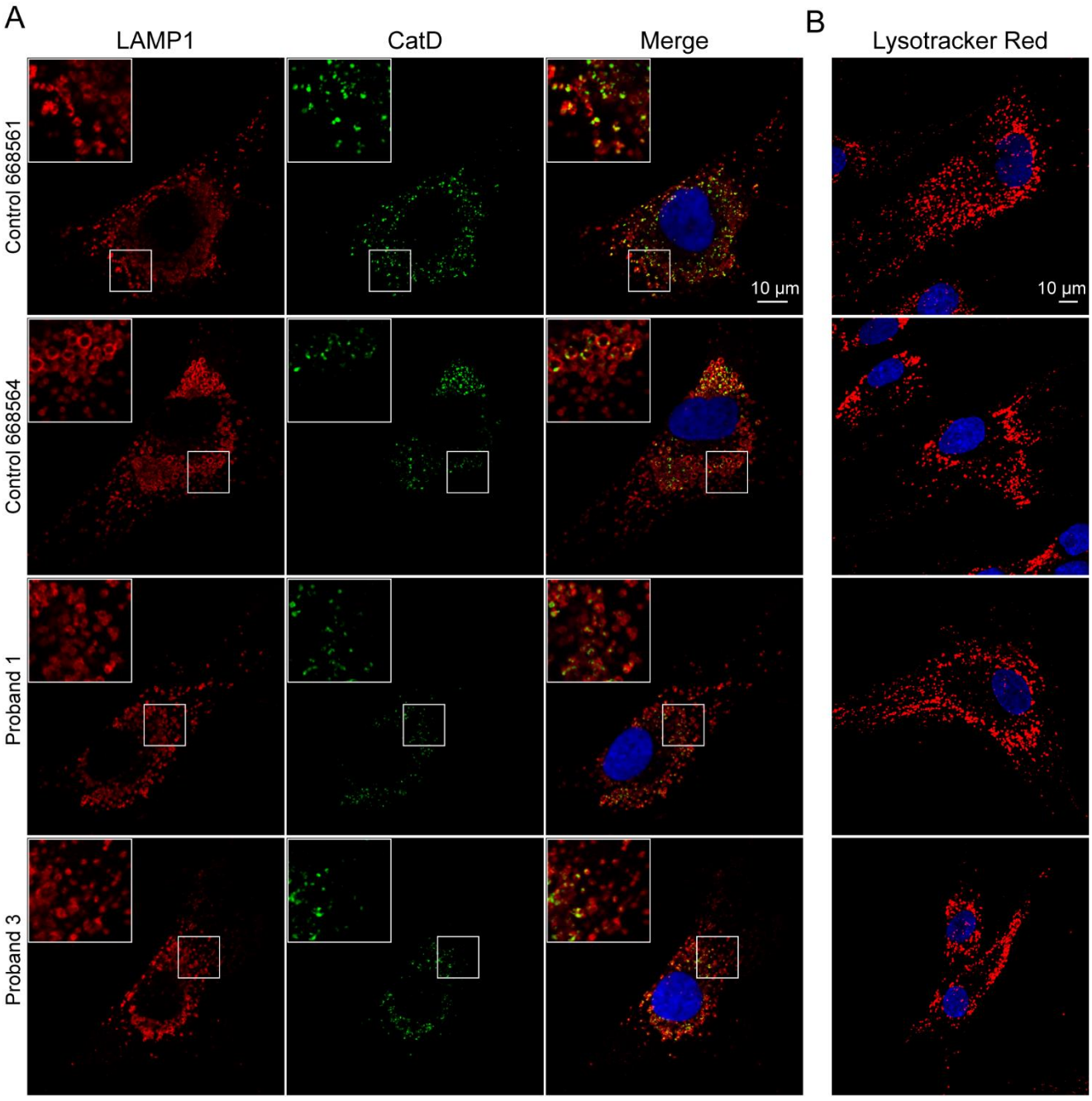

Figure S6. Primary fibroblasts of subjects heterozygous for the CIC-6 p.Tyr553Cys amino acid substitution show normal lysosomal morphology. (**A**) Fibroblasts from Subjects 1 and 3, and those from two unrelated unaffected individuals labeled for LAMP1 and cathepsin D (CatD). (**B**) Labeling with LysoTracker Red reveals no difference.

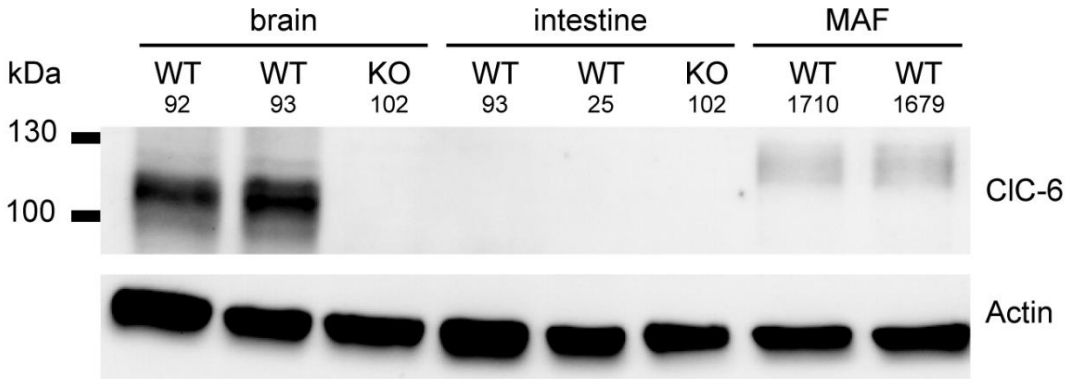

Figure S7. Western blot analysis of ClC-6 protein levels in selected mouse tissues and cells. ClC-6 is prominently detected in brain, but seems to be absent from intestine and is barely detectable in MAFs (mouse adult fibroblasts) if the faint band represents a more highly glycosylated form of ClC-6. Brain from *Clcn6*$^{-/-}$ mice[12] was taken as negative control for the previously described[12] antibody directed against an amino-terminal petipde of ClC-6. Numbers refer to individual mice or MAF preparations.

Table S1. WES statistics and data output.

Subject 1 (trio-based analysis)	
WES enrichment kit	SureSelect Human All Exon v4
Sequencing platform	Illumina HiSeq 2000
Target regions coverage >10x	96.7%
Target regions coverage >20x	92.5%
Average depth on target	57x
Total number of high-quality variants	92,873
Number of variants with predicted functional effect[1]	13,069
Private, clinically associated, and unknown/low frequency variants[2]	282
Putative disease genes (recessive trait)[3]	7[4]
- Filtered candidate genes	none
Putative disease genes (dominant trait)[3]	2[5]
- Filtered candidate genes	*CLCN6*
Subject 2 (trio-based analysis)	
WES enrichment kit	SureSelect Human All Exon v6
Sequencing platform	Illumina NovaSeq 6000
Target regions coverage >10x	97.1%
Target regions coverage >20x	96.7%
Average depth on target	151x
Total number of high-quality variants	2,125,193
Number of variants with predicted functional effect[1]	12,247
Private, clinically associated, and unknown/low frequency variants[2]	536
Putative disease genes (recessive trait)[3]	0
- Filtered candidate genes[3]	none
Putative disease genes (dominant trait)[3]	3[6]
- Filtered candidate genes	*CLCN6*
Subject 3 (trio-based analysis)	
WES enrichment kit	IDT xGen Exome Res. Panel v1.0
Sequencing platform	Illumina HiSeq 2500
Target regions coverage >10x	98.6%
Target regions coverage >20x	98.3%
Average depth on target	120x
Total number of high-quality variants	1,764,275
Number of variants with predicted functional effect[1]	12,456
Novel, clinically associated, and unknown/low frequency variants[2]	188
Putative disease genes (recessive trait)[3]	1[7]
- Filtered candidate genes[3]	none
Putative disease genes (dominant trait)[3]	3[8]
- Filtered candidate genes	*CLCN6*

[1]High-quality, non-synonymous SNVs/indels within coding exons and splice regions (-3/+8) (subject 1); high-quality SNVs/indels within coding exons and splice regions (-/+10) (subject 2); high-quality SNVs/indels within coding exons and splice regions (-/+12) (subject 3).

[2]High-quality, non-synonymous SNVs/indels within coding exons and splice regions (-/+8) with gnomAD MAF <0.1% and frequency <1% in our in-house database (~1,700 population-matched exomes) (subject 1); high-quality SNVs/indels within coding exons and splice regions (-/+10) with gnomAD MAF <0.1% (subject 2); high-quality SNVs/indels within coding exons and splice regions (-/+12) with gnomAD MAF <0.1% (subject 3).

[3]Functional impact assessed by Combined Annotation Dependent Depletion (CADD) v.1.4 (http://cadd.gs.washington.edu/), dbNSFP Mendelian Clinically Applicable Pathogenicity (M-CAP) v.1.0 (http://bejerano.stanford.edu/mcap/) and Intervar (http://wintervar.wglab.org) v2.0.1. Variants predicted as benign or likely benign by Intervar were discarded and only those with CADD score >15 or M-CAP score>0.025 were retained (subject 1); Functional impact assessed by Combined Annotation Dependent Depletion (CADD) v.1.4 (http://cadd.gs.washington.edu/), and dbNSFP Mendelian Clinically Applicable Pathogenicity (M-CAP) v.1.0 (http://bejerano.stanford.edu/mcap/). Variants with CADD score >15 and/or M-CAP score >0.025 were retained (subject 2); Functional impact assessed by Combined Annotation Dependent Depletion (CADD) v.1.4 (http://cadd.gs.washington.edu/), dbNSFP Mendelian Clinically Applicable Pathogenicity (M-CAP) v.1.0 (http://bejerano.stanford.edu/mcap/), and dbNSFP Rare Exome Variant Ensemble Learner (REVEL) (https://sites.google.com/site/revelgenomics/). Variants with CADD score >25, M-CAP score >0.05, and/or REVEL > .100 were retained (subject 3).

[4]*NID1* (c.3038C>A; p.Thr1013Asn, M-CAP=0.065), *ERO1B* (c.37G>C, p.Gly13Arg, CADD=17.52, M-CAP=0.078), *PPP2R3A* (c.680C>T, p.Thr848Met, CADD=34), *DMTN* (c.896G>C, p.Ser299Thr, CADD=16.32), *FAM120C* (c.2600G>A, p.Arg867Gln, CADD=23.3), *ZDHHC15* (c.1004C>T, p.Thr335Met, CADD=16), *DRP2* (c.844T>C, p.Phe282Leu, CADD=17.92).

[5] *CLCN6* (c.1658A>G, p.Tyr553Cys, CADD=28.3, M-CAP=0.48), *FKBP6* (c.616G>C, p.Ala206Pro, CADD= 15.4, M-CAP=0.045).

[6] *CLCN6* (c.1658A>G, p.Tyr553Cys, CADD=28.3, M-CAP=0.48), *NF1* (c.2452delT, p.Ser818Phefs*3), *TMTC3* (c.1712A>C, p.Glu571Ala, CADD=25, M-CAP= 0.058).

[7]*SLC6A19* (c.898G>A, p.Glu300Lys; CADD=23.5, M-CAP=.098, REVEL=.453, and c.941C>T, p.Ser314Leu; CADD=26.2, M-CAP=.235, REVEL=.788).

[8] *CLCN6* (c.1658A>G, p.Tyr553Cys, CADD=28.3, M-CAP=0.48, REVEL=.959); *COQ3* (c.523G>A, p.Asp175Asn, CADD=34, M-CAP=.122, REVEL=.585); *GUSB* (c.290G>T, p.Gly97Val, CADD=26.3, M-CAP=644, REVEL=.945).

Table S2. Clinical features of the three subjects included in the study.

	HPO terms	Subject 1 (family 1)	Subject 2 (family 2)	Subject 3 (family 3)
Gene		*CLCN6*	*CLCN6*	*CLCN6*
Mutation (NM_001286.3)		c.1658A>G, p.Tyr553Cys	c.1658A>G, p.Tyr553Cys	c.1658A>G, p.Tyr553Cys
Origin		*de novo*	*de novo*	*de novo*
Ethnic background		European descent	European descent	European descent
Sex		Male	Female	Female
Clinical Features				
Pregnancy		Uneventful	Reduced fetal movements	Uneventful
Birth at (weeks of gestation)		40	39+6	37+3
Birth weight (g) (centile, z-score)		NA	3,880 (84, 1.01)	2,636 (8, -1.34)
Birth length cm (centile, z-score)		NA	50 (23, -0.73)	47 (12, -1.2)
OFC birth cm (centile, z-score)		NA	35 (54, 0.11)	NA
Last examination				
Age		Alive, 6 y 4 m	22 m; deceased at 23 m	Alive, 18 m
Weight kg (centile, z-score)		20.0 (50, -0.63)	12.6 (70, 0.52)	9.5 (20, -0.84)
Height cm (centile, z-score)		100 (<1, -3.62)	87 (64, 0.37)	74.4 (<1, -2.57)
BMI (centile, z-score)		20 (96.9, 1.9)	16.6 (67, 0.43)	17.14 (85, 1.04)
OFC cm (centile, z-score)		50 (7, -1.42)	48 (47, -0.07)	46.8 (59, +0.24)
Neurological features				
Global developmental delay	HP:0001263	Severe DD noted at 5 m with regression at 6 m (loss of speech and motor function)	Global DD with regression (loss of speech and motor function)	Global developmental delay with regression at 6 m
Motor development	HP:0001270	Absence of spontaneous movements	Rolling over, but no crawling, sitting and standing at 13 m	Sitting unsupported at 14 m; cruises with help
Speech impairment	HP:0002167	Absent language	Single words	Babbles, verbalizes 7 to 8 words
Muscular hypotonia	HP:0001252	Generalized hypotonia; apostural quadriplegia	Severe truncal hypotonia, no spasticity	Generalized hypotonia (truncal>appendicular)
Movement disorder	HP:0100022	N	Intermittent severe choreoathetoid, dyskinetic movement disorder, loss of coughing and swallowing reflexes at 16 m	N
Seizures	HP:0001250	N	N	N
EEG features	HP:0002353	Frontal epileptic abnormal-lities (5 m). Slow disorganized background activity, with slower centro-posterior bilateral waves; absence of epileptiform abnormalities (6 y 4 m)	Loss of normal background activity and structure with frequency slowing, no epileptic discharges (20 m)	Video EEG x2 negative (7 m)
MRI scan		Bilateral symmetrical region at level of corticospinal tracts, in correspondence of the cerebral peduncles, substantia nigra, thalami and dorsal brainstem with restricted diffusion at DWI. Mild fronto-temporal atrophy. Bilateral fronto-parietal subdural hematomas (10 m). Widespread signal abnormalities (reduction in the representation of the deep white substance in particular posterior, periventricular and at level of the posterior arm of the internal capsule: volumetric	Normal (5 m) Mild cerebral atrophy and bilateral diffusion restriction in the upper cerebellar peduncles and dorsal brainstem (18 m) MRS not assessed.	Diffusion restriction involving bilateral cerebral peduncles, dorsal midbrain and inferiorly along the dorsal aspect of the pons and medulla, with mild T2 hyperintensity (7 m). MRS: lactate peaks within the left parietal subcortical matter & frontal horns (18 m). Repeat MRI/MRS at 23 m: improved diffusion restriction with small persistent foci of restricted diffusion in the bilateral anteromedial cerebral peduncles. No evidence of lactate peak but small GLX peak present, which is nonspecific, but could be seen in the setting of hepatic dysfunction.

		reduction of thalami with bilateral symmetrical thalamic FLAIR hyper-intensity. Brainstem and spinal cord hypoplasia (6 y 4 m). Normal MRS (6 y 4 m).		
Neurogenic bladder	HP:0000011	Y	Y suprapubic catheter at 19 m	N
Abnormality of temperature regulation	HP:0004370	Y (hyperthermia)	Y (during crisis, severe hyperthermia)	N
Other clinical findings				
Cardiovascular system abnormality	HP:0030680	Normal	Normal	Normal
Hearing abnormality	HP:0000364	Normal	Normal	Normal
Abnormality of vision	HP:0000504	Cortical blindness with wandering ocular movements	Nystagmus and loss of fixation (fundoscopy with optic disc elevation and neuroretinal rim pallor)	Optic disc elevation (bilateral); alternating esotropia and strabismic amblyopia
Abnormality of the respiratory system	HP:0002086	Chronic respiratory insufficiency, tracheostomy	Chronic respiratory insufficiency, tracheostomy at the age of 19 m	Chronic respiratory insufficiency, tracheostomy & ventilator dependent since 6 m
Abnormality of the skin	HP:0000951	Insensitivity to pain, hyperhidrosis, trichorrhexis nodosa: reduced hair copper content	Hyperhidrosis	N
Feeding difficulties	HP:0011968	Severe dysphagia; exclusive by gastrostomy (PEG)	Failure to thrive, poor feeding and need for gastrostomy	Required G tube feeding for 3 m
Craniofacial features	HP:0001999	Hypertelorism, arched eyebrows, long philtrum, thin upper lip	N	N
Other molecular findings		none	Neurofibromatosis type 1 (*NF1*:NM_000267.3: c.2452delT (p.S818Pfs*3), *de novo*	*SLC6A19*: c.941C>T (p.S314L) paternally-inherited; c.898G>A (p.E300K) maternally-inherited; aminoaciduria
Electrophysiology studies				
VEPs		Increased latency and abnormal morphology of P100 wave	NA	NA
ERG		Normal	NA	NA
BAEPs		Normal	NA	NA
Skin biopsy		Abnormal elastic fibers	NA	NA
Muscle biopsy		Mild signs of myopathy; abnormal variation in muscle fiber sizes with very small type 1 fibers and prevalence of type 2 fibers	Signs of myopathy, sub-sarcolemmal accumulation of degenerated mito-chondria and fatty vacuoles. No COX negative fibers	H&E showed abnormal variation in muscle fiber sizes with many scattered very small type II muscle fibers. EM still pending
Nerve conduction studies		SPN	SPN	Normal
Biochemistry				
Copper (µg/dL)		5.0; 13; 24; 25 (nv 80 -180); 62.6 (under copper suppl.)	NA	130 (nv 80-180)
Ceruloplasmin (mg/dL)		24-26 (nv 20-60)	NA	Normal
Copper excretion (µg/24h)		15.4 (nv 15-70)	NA	NA
VLCFA		Normal	NA	NA
Blood Lactate (mM)		Normal	Normal	Normal
CSF Lactate (mM)		NA	Normal	Normal
Plasma Alanine (µmol/L)		531 (nv 150-400)	Normal	Normal
Plasma Creatine (µmol/L)		117 – 140 (nv 16-93)	Normal	NA

[#]Copper/Creat Ratio <5 µg/g Creatinine (urine spot). Normal values were not determined for this age.
Female > or =18 years: 7-72 µg/g creatinine.

BAEPs, brainstem auditory evoked potentials; CSF, cerebrospinal fluid; DD, developmental delay; ERG, electroretinography; m, months; MRS, magnetic resonance spectroscopy; N, feature absent; NA, not assessed; nv, normal value(s); SPN, Sensory peripheral neuropathy; VEP, visual evoked potentials; VLCFA, very long chain fatty acid; Y, feature present; y, years.

Supplemental Methods

Genomic analyses

DNA of the subjects and their parents was extracted from leukocytes by standard procedures for a trio-based whole-exome sequencing (WES) analysis.

For subject 1, exome capture was carried out using SureSelect Human All Exon v4 (Agilent), and sequencing was performed using a NextSeq500 platform (Illumina). Raw data were processed and analyzed using an in-house implemented pipeline previously described, which is based on the GATK Best Practices.[1] The UCSC GRCh37/hg19 version of genome assembly was used as a reference for reads alignment by means of BWA-MEM tool,[2] and the subsequent variant calling with HaplotypeCaller (GATK v3.7).[1] We used SnpEff v.4.3[3] and dbNSFP v.3.5[4] tools for variants functional annotation, including Combined Annotation Dependent Depletion (CADD) v.1.4,[5] Mendelian Clinically Applicable Pathogenicity (M-CAP) v.1.0,[6] and Intervar v.2.0.1[7] for functional impact prediction. Thereby, the analysis was narrowed to variants that either affect coding sequences or splice site regions. High-quality variants were filtered against public databases (dbSNP150 and gnomAD V.2.0.1) so that only variants with unknown frequency or having MAF <0.1%, as well as variants occurring with frequency <1% in our population-matched database (~1700 WES) were considered.

For subject 2, enrichment was carried out using the SureSelect Human All Exon V6 kit (Agilent). Each captured library was then loaded and sequenced on the HiSeq platform (Illumina). Variant analysis was performed as previously described,[8,9] using GATK.[10] Afterwards, variants were functionally annotated and compared to those documented in publicly accessible genetic variant databases (dbSNP138, 1,000 Genomes, and ExAC) using ANNOVAR (v2017-07-17).[11] Only exonic and intronic variants that were private (absent in public database), rare (with a MAF <0.1% and no homozygotes in public databases) and located at exon-intron boundaries ranging from -10 to +10 were retained.

For subject 3, exome capture and sequencing were performed clinically at GeneDx (Gaithersburg, MD, USA). Exome capture was carried out using the IDT xGen Exome Research Panel v1.0, and sequenced on an Illumina Hiseq 2500. Variants were annotated with ANNOVAR (v2019-10-24)[11] and filtered against public databases (< 1%MAF, GnomAD v2.0.1 and v3.0). Variants in coding regions and splice regions were assessed for functionality using CADD, M-CAP, and REVEL scores within ANNOVAR.

Sequence validation and segregation analyses of all candidate variants were performed by Sanger-sequencing. Primer pairs designed to amplify the coding exons of interest and PCR conditions are available on request. Amplicons were directly sequenced using the ABI BigDye Terminator Sequencing kit (Applied Biosystems) and an automated capillary sequencer (ABI 3500/SeqStudio, Applied Biosystems).

Western blot analysis

Lysates from membrane preparations from brain and intestine form WT and *Clcn6*$^{-/-}$ mice, [12] or from WT mouse adult fibroblasts, were separated by SDS PAGE (30 µg protein per lane), blotted, and probed

with a previously described anti-ClC-6 antibody.[12] SuperSignal West Pico Plus (Thermo Fisher) was used for detection.

Supplemental References

1. Van der Auwera, G.A., Carneiro, M.O., Hartl, C., Poplin, R., Del Angel, G., Levy-Moonshine, A., Jordan, T., Shakir, K., Roazen, D., Thibault, J., et al. (2013). From FastQ data to high confidence variant calls: the Genome Analysis Toolkit best practices pipeline. Current protocols in bioinformatics 43, 11 10 11-11 10 33.
2. Li, H., and Durbin, R. (2009). Fast and accurate short read alignment with Burrows-Wheeler transform. Bioinformatics 25, 1754-1760.
3. Cingolani, P., Platts, A., Wang le, L., Coon, M., Nguyen, T., Wang, L., Land, S.J., Lu, X., and Ruden, D.M. (2012). A program for annotating and predicting the effects of single nucleotide polymorphisms, SnpEff: SNPs in the genome of Drosophila melanogaster strain w1118; iso-2; iso-3. Fly 6, 80-92.
4. Liu, X., Jian, X., and Boerwinkle, E. (2013). dbNSFP v2.0: a database of human non-synonymous SNVs and their functional predictions and annotations. Hum Mutat 34, E2393-2402.
5. Kircher, M., Witten, D.M., Jain, P., O'Roak, B.J., Cooper, G.M., and Shendure, J. (2014). A general framework for estimating the relative pathogenicity of human genetic variants. Nat Genet 46, 310-315.
6. Jagadeesh, K.A., Wenger, A.M., Berger, M.J., Guturu, H., Stenson, P.D., Cooper, D.N., Bernstein, J.A., and Bejerano, G. (2016). M-CAP eliminates a majority of variants of uncertain significance in clinical exomes at high sensitivity. Nat Genet 48, 1581-1586.
7. Li, Q., and Wang, K. (2017). InterVar: Clinical Interpretation of Genetic Variants by the 2015 ACMG-AMP Guidelines. Am J Hum Genet 100, 267-280.
8. Kortüm, F., Caputo, V., Bauer, C.K., Stella, L., Ciolfi, A., Alawi, M., Bocchinfuso, G., Flex, E., Paolacci, S., Dentici, M.L., et al. (2015). Mutations in *KCNH1* and *ATP6V1B2* cause Zimmermann-Laband syndrome. Nat Genet 47, 661-667.
9. Girisha, K.M., Kortüm, F., Shah, H., Alawi, M., Dalal, A., Bhavani, G.S., and Kutsche, K. (2016). A novel multiple joint dislocation syndrome associated with a homozygous nonsense variant in the *EXOC6B* gene. Eur J Hum Genet 24, 1206-1210.
10. McKenna, A., Hanna, M., Banks, E., Sivachenko, A., Cibulskis, K., Kernytsky, A., Garimella, K., Altshuler, D., Gabriel, S., Daly, M., et al. (2010). The Genome Analysis Toolkit: a MapReduce framework for analyzing next-generation DNA sequencing data. Genome research 20, 1297-1303.
11. Wang, K., Li, M., and Hakonarson, H. (2010). ANNOVAR: functional annotation of genetic variants from high-throughput sequencing data. Nucleic Acids Res 38, e164.
12. Poët, M., Kornak, U., Schweizer, M., Zdebik, A.A., Scheel, O., Hoelter, S., Wurst, W., Schmitt, A., Fuhrmann, J.C., Planells-Cases, R., et al. (2006). Lysosomal storage disease upon disruption of the neuronal chloride transport protein ClC-6. Proc Natl Acad Sci U S A 103, 13854-13859.